







# Acceleration Feedback Controller Processor Design of a Segway

Ronal P. Chand <sup>†,\*</sup>, Ravinesh Chand <sup>†</sup>, Mansour Assaf <sup>‡</sup>,  
Shailendra V. Narayan <sup>†</sup>, Parmesh R. Naicker <sup>†</sup> and Vimi Kapadia <sup>†</sup>

**Abstract**—Traffic congestions and carbon emissions are a few contributing factors to various problems in large cities across the globe. This paper provides the Single Purpose Processor (SPP) design for a nonholonomic segway robot's acceleration feedback control laws. The acceleration control rules are derived from the total potentials generated by the Lyapunov-based Control Scheme (LbCS), which were validated using Wolfram Mathematica simulation software. Due to the robot autonomously, the riders can have a safe ride while reaching their destination. Furthermore, the design could be implemented for rapid prototyping in hardware such as a VLSI chip, an ASIC chip, or an FPGA board. Hence, the segway robot could be used as a personal transport that could be ridden on narrow paths such as pavements while consuming less energy when compared to larger vehicles and help reduce carbon emissions; thus, the segway robot could be seen as an essential personal transport to contribute towards smart city goals.

**Index Terms**—Segway, Artificial potential fields, Obstacle avoidance, Acceleration feedback controller, Processor design

## I. INTRODUCTION

Information and communication technology (ICT) has grown substantially, assisting development in various sectors like education [1], agriculture [2], transportation, healthcare [3], good governance, and data security [4] by lowering the cost, pollution and dependency of others. Technological advancements have made it possible to connect computers, mobile devices such as phones, automated vehicles, and people to communicate in a networked environment to work collaboratively. In addition, these advancements have provided various manufacturing industries with rapid insight into essential processes. Autonomous vehicles, social robots [5], humanoids [6], industrial robots [7], and medical robots [8] are a few different types of robots. Furthermore, smaller vehicles such as hoverboards, e-scooters, motorbikes, and segways can contribute to solving various city problems such as traffic congestion and pollution. This research focuses on the specific area of transportation robots, which deals with the control and design of autonomous segway.

A segway is a two-wheeled self-balancing personal transporter. The segway's upright position is maintained via on-board computers, sensors, and motors. Segways as personal

transport would provide a greener environment as it requires less energy when compared to larger vehicles. Smaller vehicles can be utilized on narrow paths such as pavements and within buildings efficiently. Segways could be utilized in a smart city setting, where efficient communication from ICT and IoT can provide data for optimized decisions, which help solve various city problems. Various applications with segways are possible such as courier services, security patrols, and personal transport to work. However, James Heselden, former owner of "Segway Inc.," was pronounced deceased after falling from the cliff while riding a Segway [9]. Segway accidents that resulted in fractures and concussions have also been reported in [10]. The major problem with segway was not its make, rather its controllability. The invention, where a rider takes full control to move segway forward, back, and completely stop it, has caused failures because of human error. Thus, there is a clear indication to improve segways for a more reliable and safer ride.

Several aspects of segway control are discussed in [11] such as sensor data fusion, noise filtering, and time lag in gathering and transferring data. The algorithm and sequence of control such as data monitoring and experimentation was by the Real Time (RT) controller. Furthermore, using Lyapunov's feedback control design technique, Maddahi et al. [12] conducted research on segways in which they designed discontinuous controllers for a segway and demonstrated the stability of the proposed system. Authors of [13] derived nonlinear equations of motion for the segway by employing the Krupková method for a practical mechanical system. A numerical solution of the reduced equation was presented numerically using nonlinear reduced dynamics modeling with a simulation of a two-wheeled self-balancing mobile robot system. In [14], a Balbot robot was studied for its ability to balance while following a line. The authors used visual servoing and sensor fusion techniques that enabled the robot to follow the floor line acquired by a camera as the desired path, and controllers were developed to offer superior line tracking and balancing performance.

One of the major tasks in prototyping a robot after validating it through simulations is the design of its controller and implementing on processor using a hardware descriptive language. Processors are chips or logic circuits that receive, reply to, and carry out the fundamental instructions of a machine. General purpose processors (GPP), special purpose processors (SPP), and application-specific instruction set processors (ASIP) are different forms of embedded processors. In this paper, the

<sup>‡</sup> School of Information Technology, Engineering, Mathematics & Physics, The University of the South Pacific, Suva, Fiji.

<sup>†</sup> School of Mathematical & Computing Sciences, Fiji National University, Suva, Fiji.

\*Corresponding author email:  
ronal.chand@fnu.ac.fj

development of the special purpose processors (SPP) design of a proposed nonholonomic autonomous segway robot for acceleration-based feedback control laws is presented which could be implemented in hardware like VLSI chip, ASIC or an FPGA board for fast prototyping. The control laws are derived from a total potential using Lyapunov-based Control Scheme (LbCS) [15]–[33] and verified using computer simulation. This paper is based on theoretical exposition as all the information communication is virtual and can be easily compared to real-life data. The presented segway robot could be used for personal transport, which can assist in solving city problems such as traffic congestion and pollution.

## II. SYSTEM MODELLING

Consider a two-wheel self-balancing segway robot as shown in Figure 1. The center of the mass of the segway has a cartesian coordinate of  $(x, y)$ . The steering wheel is at a distance of  $\lambda$ , with  $\theta$  begin the orientational angle of the segway respect to  $z_1$ -axis from the center of the two diametrically opposed wheels. The horizontal distance between the center of the two wheels is  $\delta$  with the wheel's radius being  $r$ , and we consider an imaginary point  $\epsilon$  from the center of mass with an orientational angle  $\theta$  as shown in Figure 1. The left and right wheel angular velocities are denoted as  $\dot{\phi}_L = v_L$  and  $\dot{\phi}_R = v_R$ , respectively. The system could be represented by the vector notation as

$$\mathbf{x} = (x, y, \theta, \phi_R, \phi_L, v_R, v_L) \in \mathbb{R}^7 \quad (1)$$

to refer to the various position and velocities of the segway robot. The robot is assumed to have a pure rolling of the two driven wheels with respect to  $(x, y) \in \mathbb{R}^2$  thus the kinematic model is represented as

$$\left. \begin{aligned} \dot{x} &= \frac{r}{2}(v_R + v_L) \cos \theta + \frac{r\lambda}{2\delta}(v_R - v_L) \sin \theta \\ \dot{y} &= \frac{r}{2}(v_R + v_L) \sin \theta + \frac{r\lambda}{2\delta}(v_R - v_L) \cos \theta \\ \dot{\theta} &= \frac{r}{2\delta}(v_R - v_L), \\ \dot{\phi}_L &= v_L, \dot{\phi}_R = v_R, \dot{v}_R = a_R, \dot{v}_L = a_L. \end{aligned} \right\} \quad (2)$$

## III. ACCELERATION CONTROLLERS

In this research, the segway robot has two degrees of freedom in two-dimensional space, namely translational and rotational motion of the body with respect to the horizontal plane. Furthermore, since the segway's motion is autonomous, the pendulum bar is assumed to be rigid.

*Definition 3.1:* The target for the segway robot is  $\mathbf{x}_\tau = (a, b)$ . It is a disk with center  $(a, b)$  and radius  $r_\psi$ . It is described as the set

$$\tau := \{(z_1, z_2) \in \mathbb{R}^2 : (z_1 - a)^2 + (z_2 - b)^2 \leq r_\psi^2\}. \quad (3)$$

*Definition 3.2:* The  $n^{\text{th}}$  solid stationary obstacle is a disk with center  $\mathbf{x}_{O_n} = (o_{x_n}, o_{y_n})$  and radius  $r_{o_n} > 0$ . It is described as the set

$$O_n := \{(z_1, z_2) \in \mathbb{R}^2 : (z_1 - o_{x_n})^2 + (z_2 - o_{y_n})^2 \leq r_{o_n}^2\}. \quad (4)$$

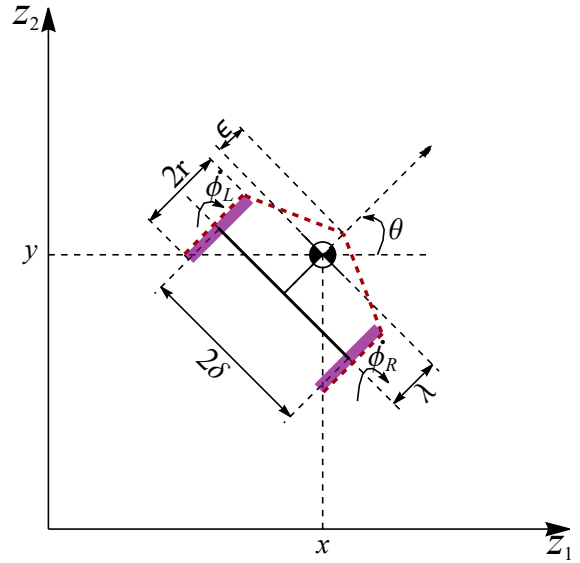


Fig. 1. Model of a Segway, a two-wheeled self-balancing robot at an orientational  $\theta$ .

### A. Attractive and Avoidance functions

The following functions have been developed as the attractive and repulsive functions which will be utilized later to develop Lyapunov function:

1) *Target Attraction:* A radically unbounded target attraction function that will ensure that the segway robot converges to its target is designed as follows

$$T(\mathbf{x}) := \frac{1}{2} \left( (x - a)^2 + (y - b)^2 + v_R^2 + v_L^2 \right). \quad (5)$$

2) *Artificial Obstacles:* There are limitations placed on the two wheels' angular velocities due to their application in practical situations. The limitations on the velocities of the wheels can only be incorporated in LbCS using artificial obstacles. The angular velocity of the right and left wheel could be bonded as  $|v_R(t)| \leq v_{max}$  and  $|v_L(t)| \leq v_{max}$ , where  $v_{max}$  is assumed to be maximum angular velocity of the two wheels. For the restrictions on velocities that would be used in the repulsive potentials, the following avoidance functions are constructed:

$$W_1(\mathbf{x}) = \frac{1}{2} (v_{max}^2 - v_R^2) \quad (6a)$$

$$W_2(\mathbf{x}) = \frac{1}{2} (v_{max}^2 - v_L^2) \quad (6b)$$

3) *Stationary Obstacles Avoidance:* For the segway robot to avoid  $n^{\text{th}}$  stationary obstacles for  $n \in (1, 2, 3, \dots, q)$  and  $j \in (1, 2)$  the nearest point of the segway robot that is closest to the obstacle defined by equation (4) is considered using minimum distance technique (MDT). The distance functions is given by

$$D_j = \|(X_j, Y_j) - \mathbf{x}_{O_n}\|.$$

The segway could be enclosed by four lines segments, which are shown in dashed red lines in Figure 1. To avoid  $n^{\text{th}}$

stationary solid obstacle with center  $(o_{x_n}, o_{y_n})$ , radius of  $r_{o_n}$  where  $n \in 1, 2, 3, \dots, q$  and  $j \in 1, 2$ , the following obstacle avoidance function is adopted:

$$W_{jn}(x) = \frac{1}{2}[(X_j + 2r\chi_{jn} \cos \theta - o_{x_n})^2 + (Y_j + 2r\chi_{jn} \sin \theta - o_{y_n})^2 - r_{o_n}^2] \quad (7)$$

and

$$W_{jn}^*(x) = \frac{1}{2}[(X_j + 2r \cos \theta + \gamma_{jn}(x + \epsilon \cos \theta - X_j - 2r \cos \theta) - o_{x_n})^2 + (Y_j + 2r \sin \theta + \gamma_{jn}(y + \epsilon \sin \theta - Y_j - 2r \sin \theta) - o_{y_n})^2 - r_{o_n}^2] \quad (8)$$

where

$$X_j = x - (r + \lambda) \cos \theta + (-1)^j \delta \sin \theta,$$

and

$$Y_j = y - (r + \lambda) \sin \theta - (-1)^j \delta \cos \theta.$$

It is noted that

$$\chi_{jn} = \min\{\max\{0, \Phi\}, 1\}$$

and

$$\gamma_{jn} = \min\{\max\{0, \Omega\}, 1\}.$$

Moreover,  $\Phi$  and  $\Omega$  are as follows:

$$\Phi = \frac{\lambda + r + (o_{x_n} - x) \cos \theta + (o_{y_n} - y) \sin \theta}{2r}$$

and

$$\Omega = \frac{\delta^2 + (\lambda - r)(\lambda - r + \epsilon) + A \cos \theta + B \sin \theta}{\delta^2 + (\lambda - r + \epsilon)^2},$$

where  $A = (-1)^j \delta (o_{y_n} - y) + (o_{x_n} - x)(\lambda - r + \epsilon)$  and  $B = (-1)^j \delta (-o_{x_n} + x) + (o_{y_n} - y)(\lambda - r + \epsilon)$ .

4) *Auxiliary function:* The following auxiliary function is provided to ensure that the nonlinear acceleration controllers vanish at the target:

$$R(\mathbf{x}) = \frac{1}{2}((x - a)^2 + (y - b)^2). \quad (9)$$

### B. A Lyapunov Function

Let  $\alpha_1, \alpha_2, \beta_{jL}$  and  $\beta_{jn}^*$  be positive constants then the Lyapunov function suppressing  $t$  of system (2) becomes

$$L(\mathbf{x}) = T(\mathbf{x}) + R(\mathbf{x}) \sum_{k=1}^2 \frac{\alpha_k}{W_k(\mathbf{x})} + R(\mathbf{x}) \sum_{j=1}^2 \sum_{n=1}^q \left( \frac{\beta_{jn}}{W_{jn}(\mathbf{x})} + \frac{\beta_{jn}^*}{W_{jn}^*(\mathbf{x})} \right). \quad (10)$$

Along a trajectory of system (2)

$$\begin{aligned} \dot{L}(x) &= \dot{T}(\mathbf{x}) + \dot{R}(\mathbf{x}) \sum_{j=1}^2 \sum_{n=1}^q \left( \frac{\beta_{jn}}{W_{jn}(\mathbf{x})} + \frac{\beta_{jn}^*}{W_{jn}^*(\mathbf{x})} \right) \\ &+ \dot{R}(\mathbf{x}) \left( \sum_{k=1}^2 \frac{\alpha_k}{W_k(\mathbf{x})} \right) - R(\mathbf{x}) \left( \sum_{k=1}^2 \frac{\alpha_k \dot{W}_k(\mathbf{x})}{W_k^2(\mathbf{x})} \right) \\ &+ R(\mathbf{x}) \left( \frac{\beta_{jn} \dot{W}_{jn}(\mathbf{x})}{W_{jn}^2(\mathbf{x})} + \frac{\beta_{jn}^* \dot{W}_{jn}^*(\mathbf{x})}{W_{jn}^{*2}(\mathbf{x})} \right). \end{aligned}$$

$\dot{L}(x)$  could be rearranged upon collecting terms  $v_R$  and  $v_L$ , as

$$\dot{L}(x) = f(x)v_R + g(x)v_L,$$

where

$$f = \frac{\partial L}{\partial x} \frac{r}{2\delta} (\delta \cos \theta - \lambda \sin \theta) + a_R \left( 1 + \frac{\alpha_1 R(\mathbf{x})}{W_1^2(\mathbf{x})} \right) + \frac{\partial L}{\partial y} \frac{r}{2\delta} (\delta \sin \theta + \lambda \cos \theta) + \frac{\partial L}{\partial \theta} \frac{r}{2\delta},$$

and

$$g = \frac{r}{2\delta} (\delta \cos \theta + \lambda \sin \theta) \frac{\partial L}{\partial x} + a_L \left( 1 + \frac{\alpha_2 R(\mathbf{x})}{W_2^2(\mathbf{x})} \right) + \frac{r}{2\delta} (\delta \sin \theta - \lambda \cos \theta) \frac{\partial L}{\partial y} - \frac{r}{2\delta} \frac{\partial L}{\partial \theta}.$$

As a result, the rear right and left wheels' angular acceleration can be characterised as follows:

$$\left. \begin{aligned} a_R &= \frac{-W_1^2(\mathbf{x})}{W_1^2(\mathbf{x}) + \alpha_1 R(\mathbf{x})} \left( \frac{r}{2\delta} \frac{\partial L}{\partial \theta} + \sigma_1 v_R \right) \\ &- \frac{W_1^2(\mathbf{x})}{W_1^2(\mathbf{x}) + \alpha_1 R(\mathbf{x})} \left( \frac{r}{2\delta} \frac{\partial L}{\partial x} \right) (\delta \cos \theta - \lambda \sin \theta) \\ &+ \frac{W_1^2(\mathbf{x})}{W_1^2(\mathbf{x}) + \alpha_1 R(\mathbf{x})} \left( \frac{r}{2\delta} \frac{\partial L}{\partial y} \right) (\delta \sin \theta + \lambda \cos \theta) \\ a_L &= \frac{-W_2^2(\mathbf{x})}{W_2^2(\mathbf{x}) + \alpha_2 R(\mathbf{x})} \left( \sigma_2 v_L - \frac{r}{2\delta} \frac{\partial L}{\partial \theta} \right) \\ &- \frac{W_2^2(\mathbf{x})}{W_2^2(\mathbf{x}) + \alpha_2 R(\mathbf{x})} \left( \frac{r}{2\delta} \frac{\partial L}{\partial x} \right) (\delta \cos \theta + \lambda \sin \theta) \\ &- \frac{W_2^2(\mathbf{x})}{W_2^2(\mathbf{x}) + \alpha_2 R(\mathbf{x})} \left( \frac{r}{2\delta} \frac{\partial L}{\partial y} \right) (\delta \sin \theta - \lambda \cos \theta). \end{aligned} \right\} \quad (11)$$

## IV. SIMULATION

The effectiveness of the LbCS and the non-linear acceleration-based controllers were verified numerically using computer simulations by the Runge-Kutta Method (RK4) technique using the Wolfram Mathematica 12.3 programme.

*Example 4.1:* Consider a segway robot moving from its initial position to a final configuration while avoiding an obstacle in its path. Table I shows the numerical values of the segway's initial states, restrictions, control and convergence parameters. The starting and final configurations of the segway robot with the stationary obstacle position are provided in Figure 2. Position and orientation of the segway robot at  $t = 0, 90, 190, 240, 300, 500$  and  $1600$  with the trajectory of the robot is shown in purple.

As time evolves, the robot comes closer to its destination, as shown in Figure 2. Figure 3 shows that  $L(\mathbf{x})$  monotonically decreasing as time evolves and its time derivative. It indicate that the segway robot is approaching its destination with respect to time. The angular velocities,  $v_R$  and  $v_L$  of the segway robot are shown in Figure 4. The right and left wheels angular velocities of the segway robot showing deceleration as it approaches the target. The segway have negative velocity  $v_R$ , indicating that the right-wheel is in reverse direction.

TABLE I

**Example 4.1.** NUMERICAL VALUES OF THE INITIAL STATES, CONSTRAINTS, AND CONTROL AND CONVERGENCE PARAMETERS OF THE SEGWAY ROBOT.

Initial Configuration	
Rectangular position	$(x_0, y_0) = (10, 10)$
Initial orientation	Randomized between $-\pi \leq \theta \leq \pi$
Constraints	
Dimensions	$\delta = 5, r = 2, \lambda = 4, \epsilon = 4$
Target location	$(a, b) = (100, 100)$
Stationary obstacle Position	$(o_{x_1}, o_{y_1}) = (50, 50)$
Radius of fixed obstacle	$r_{o_1} = 10$
Maximum angular velocities	$v_{Rmax} = v_{Lmax} = 1$
Control and Convergence parameters	
Artificial obstacle avoidance	$\alpha_1 = \alpha_2 = 0.01$
Stationary Obstacles Avoidance	$\beta_{jn} = \beta_{jn}^* = 10$
Convergence	$\sigma_1 = \sigma_2 = 500$

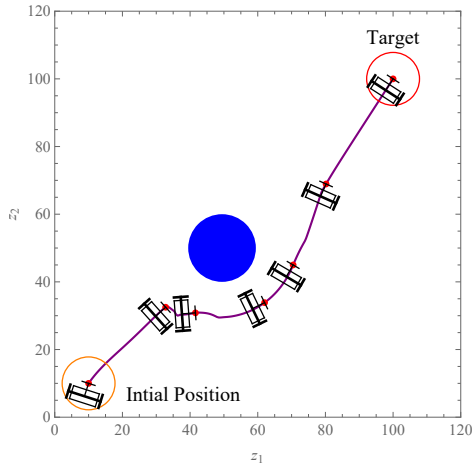


Fig. 2. Position and orientation at different times.

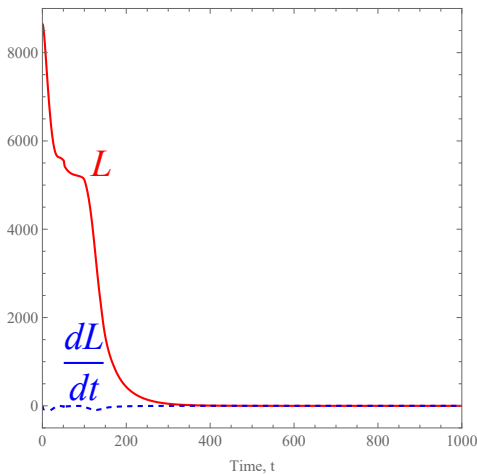


Fig. 3. Lyapunov function and its time derivative.

**Example 4.2:** This example considers the robot moving from its initial position to final position in an environment consisting of three randomly generated static obstacles. Stationary obstacle positions are randomly generated with a fixed radius

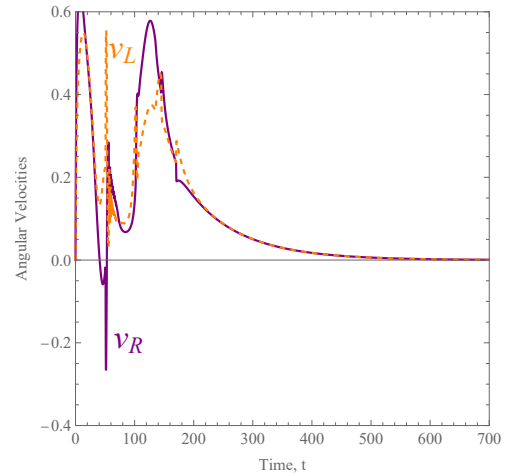
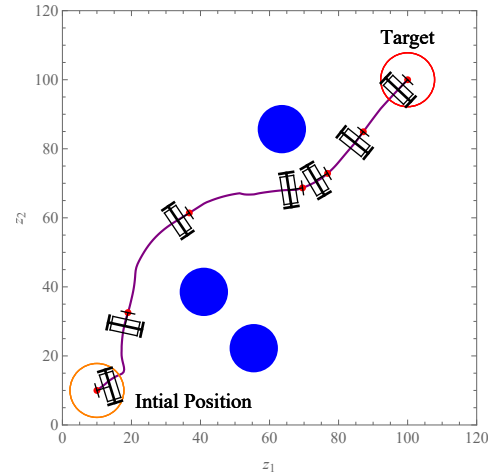


Fig. 4. Angular velocities.

of 7 units. Other initial configurations, constraints, and control parameters are kept the same as in Table I. Figure 5 shows the segway robot avoiding randomly generated static obstacles present in its path while moving from its initial position to its final destination.

Fig. 5. Position and orientation of the segway robot at  $t = 0, 40, 80, 135, 150, 190,$  and  $1600$ .

## V. ELECTRICAL DESIGN

Figure 6 provides the Acceleration Feedback Controller topology which is designed to be implemented on an FPGA board where where  $(x_0, y_0, \theta_0)$  is the initial conditions. The system constraint, the control parameters, the system outputs  $x, y, \theta, \Phi_R, \Phi_L, v_R, v_L$  are as shown in Figure 6. The design of the controller as a Single Purpose Processor (SPP) is presented in Figure 7. The embedded processor design can be implemented in hardware on a VLSI chip, ASIC, or on an FPGA board for fast prototyping. The Finite State Machine with Datapath of the control algorithm has separate unique states to identify instructions and data. Each individual state

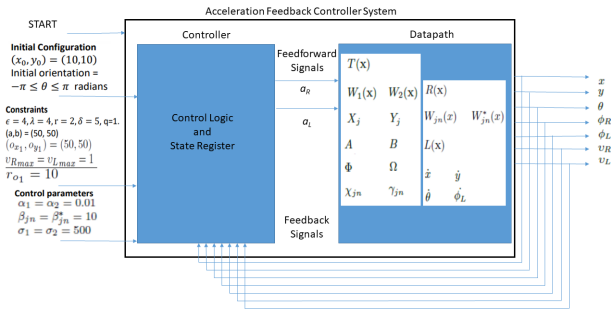
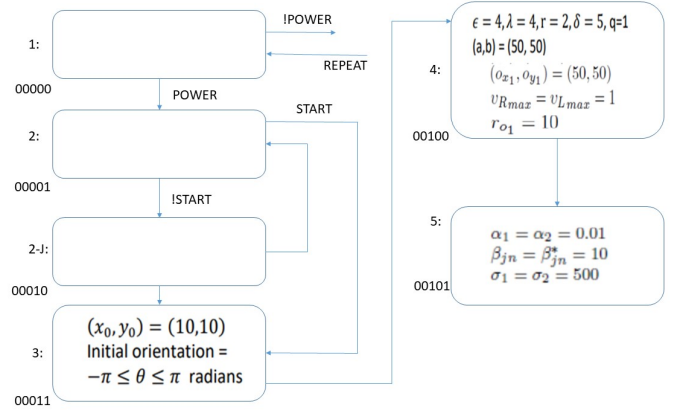


Fig. 6. The Acceleration Feedback Controller high-level Architecture

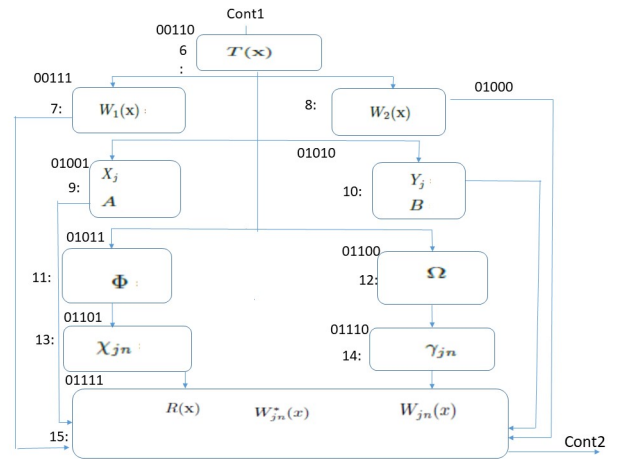
is assigned a unique binary identifier. The complete design of the system is shown in Figure 8, where data and constant parameters are replaced by registers and control signals. Input control signals such as  $x_{sel}, y_{sel}, x_{ld}, y_{ld}$  and  $z_{ld}$  are sent out by the controller to configure the logic represented by the datapath and the memory. Output control signals such as  $x_{neq_y}$  and  $x_{lt_y}$  are feedback signals returned by the datapath to the controller to indicate the status of execution of operations. The overall design consist of a control logic and state register unit (controller), the state register consists of 5 flip-flops to store the 5-bit next state of the controller,  $2 \times 1$  multiplexers to route data, two 64-bit registers, and arithmetic and logic operations (adder, subtractor, not equal and less than, etc.) capable of performing floating point operations. Multiple arithmetic/logic operators can be used to perform parallel computation to speed up the next state processing and generation.

## VI. CONCLUSION

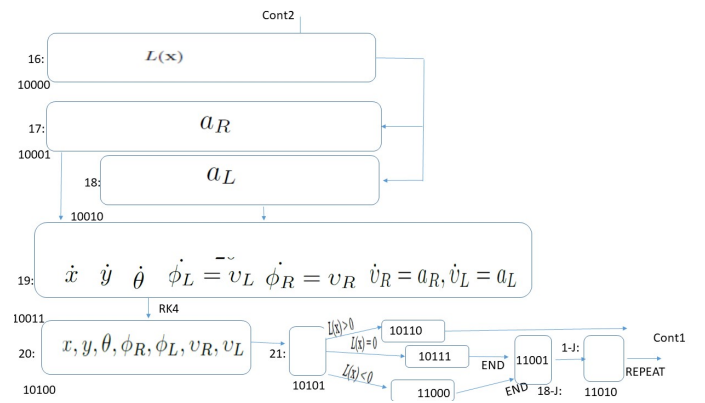
This paper provides introduces a SPP design implementation study of an autonomous segway robot. The segway robot could be utilized as a personal transport that could be ridden on a narrow path and consumes less energy when compared to larger vehicles. Segways could be seen as an essential personal transport to contribute towards smart city goals. For a comfortable ride, acceleration-based controllers of both wheels of the robot were developed using LbCS. Using the kinematic equations as part of LbCS components, the robot was shown to move from its initial position to the final target in an environment containing static obstacles using numerical proofs and computer simulations, which provided the effectiveness of the acceleration controllers. The Lyapunov-based analytical methodologies, although guaranteed to create closed-loop stability, chosen parameters may compromise the system's capacity to respond to transient changes. At the same time, the chances of algorithm singularities are also drawbacks. In the future, a hybrid system will be created by using the advantages of LbCS and choosing other heuristic methods to eliminate the disadvantages of LbCS, which can provide an asymptotic stable algorithm for the control of segway robots. The proposed segway robot's SPP processor design for acceleration feedback control laws can be implemented in hardware such as a VLSI chip, an ASIC chip, or an FPGA



(a) Stage 1



(b) Stage 2



(c) Stage 3

Fig. 7. Finite State Machine with Datapath.

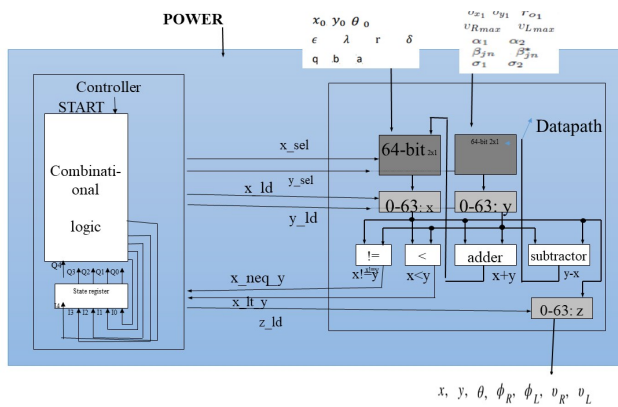


Fig. 8. Design implementation as a SPP.

board for quick prototyping. Industries can use the concept described in this paper to develop autonomous segways robots, which can be utilized in densely populated places like cities and towns for greener, faster, and safer personal transport.

#### REFERENCES

- [1] Sonia L. Critical reflections on the benefits of ICT in education. *Oxford Review of Education*, 38(1):9–24, 2012.
- [2] V.L.V. Kameswari, D. Kishore, and V. Gupta. ICTs for agricultural extension: A study in the indian himalayan region. *The Electronic Journal of Information Systems in Developing Countries*, 48(1):1–12, 2011.
- [3] Christina N. Harrington, Lyndsie Marie Koon, and Wendy A. Rogers. Chapter 17 - Design of health information and communication technologies for older adults. In Arathi S. and Farzan S., editors, *Design for Health*, pages 341–363. Academic Press, 2020.
- [4] R. Chand, M. R. Valluri, and M. Khan. Digital signature scheme over lattices. In *2021 25th International Conference on Circuits, Systems, Communications and Computers (CSCC)*, pages 71–78. IEEE, 2021.
- [5] A. Henschel, G. Laban, and E. S. Cross. What makes a robot social? A review of social robots from science fiction to a home or hospital near you. *Current Robotics Reports*, 2(1):9–19, 2021.
- [6] P. Dario, E. Guglielmelli, and C. Laschi. Humanoids and personal robots: Design and experiments. *Journal of robotic systems*, 18(12):673–690, 2001.
- [7] A. Pham and H. Ahn. High precision reducers for industrial robots driving 4th industrial revolution: state of arts, analysis, design, performance evaluation and perspective. *International journal of precision engineering and manufacturing-green technology*, 5(4):519–533, 2018.
- [8] Z. Yang and L. Zhang. Magnetic actuation systems for miniature robots: A review. *Advanced Intelligent Systems*, 2(9):2000082, 2020.
- [9] Dan C. Segway boss Jimi Heselden dies on segway: Are segways safe? - ABC News. 2010.
- [10] S. Yun, W. Lee, J.k Park, and K. Gwak. Development of a virtual environment co-simulation platform for evaluating dynamic characteristics of self-balancing personal mobility. *IEEE Transactions on Vehicular Technology*, 70(4):2969–2978, 2021.
- [11] L. J. Pinto, D. Kim, J. Y. Lee, and C. Han. Development of a segway robot for an intelligent transport system. In *2012 IEEE/SICE International Symposium on System Integration (SII)*, pages 710–715, 2012.
- [12] A. Maddahi, A. H. Shamekhi, and A. Ghaffari. A Lyapunov controller for self-balancing two-wheeled vehicles. *Robotica*, 33(1):225–239, 2015.
- [13] Soufiane H. Nonlinear reduced dynamics modelling and simulation of two-wheeled self-balancing mobile robot: Segway system. *Systems Science & Control Engineering*, 6(1):1–11, 2018.
- [14] G. Lee and S. Jung. Line tracking control of a two-wheeled mobile robot using visual feedback. *International Journal of Advanced Robotic Systems*, 10, 2013.
- [15] S. A. Kumar, J. Vanualailai, B. Sharma, A. Chaudhary, and V. Kapadia. Emergent formations of a Lagrangian swarm of unmanned ground vehicles. In *2016 14th International Conference on Control, Automation, Robotics and Vision (ICARCV)*, pages 1–6, 2016.
- [16] A. Devi, J. Vanualailai, S. A. Kumar, and B. Sharma. A cohesive and well-spaced swarm with application to unmanned aerial vehicles. In *Proceedings of the 2017 International Conference on Unmanned Aircraft Systems*, pages 698–705, Miami, FL, USA, June 2017.
- [17] S. A. Kumar, B. Sharma, J. Vanualailai, and A. Prasad. Stable switched controllers for a swarm of UGVs for hierarchal landmark navigation. *Swarm and Evolutionary Computation*, 65:100926, 2021.
- [18] S. A. Kumar, J. Vanualailai, and B. Sharma. Lyapunov functions for a planar swarm model with application to nonholonomic planar vehicles. In *2015 IEEE Conference on Control Applications (CCA)*, pages 1919–1924, 2015.
- [19] S. A. Kumar, J. Vanualailai, and B. Sharma. Lyapunov-based control for a swarm of planar nonholonomic vehicles. *Mathematics in Computer Science*, 9(4):461–475, October 2015.
- [20] A. Prasad, B. Sharma, J. Vanualailai, and S. Kumar. Motion control of an articulated mobile manipulator in 3D using the Lyapunov-based control scheme. *International Journal of Control*, pages 1–15, 2021.
- [21] S. A. Kumar, J. Vanualailai, and A. Prasad. Assistive technology: autonomous wheelchair in obstacle-ridden environment. *PeerJ Computer Science*, 7:e725:1–23, 2021.
- [22] R. Chand, S. A. Kumar, and R. P. Chand. Navigation of an n-link revolute robotic arm via hierarchal landmarks. In *2021 3rd Novel Intelligent and Leading Emerging Sciences Conference (NILES)*, pages 188–192, 2021.
- [23] R. P. Chand, S. A. Kumar, and R. Chand. LbCS navigation controllers of twining Lagrangian swarm individuals. In *2021 3rd Novel Intelligent and Leading Emerging Sciences Conference (NILES)*, pages 183–187, 2021.
- [24] S. A. Kumar, K. Chand, L. I. Paea, I. Thakur, and M. Vatikani. Herding predators using swarm intelligence. In *2021 IEEE Asia-Pacific Conference on Computer Science and Data Engineering (CSDE)*, pages 1–6, 2021.
- [25] R. P. Chand, S. A. Kumar, R. Chand, and R. Tamath. Lyapunov-based controllers of an n-link prismatic robot arm. In *2021 IEEE Asia-Pacific Conference on Computer Science and Data Engineering (CSDE)*, pages 1–5, 2021.
- [26] R. Chand, S. A. Kumar, R. P. Chand, and S. Reddy. A car-like mobile manipulator with an n-link prismatic arm. In *2021 IEEE Asia-Pacific Conference on Computer Science and Data Engineering (CSDE)*, pages 1–6, 2021.
- [27] R. Chand, R. P. Chand, and S. A. Kumar. Switch controllers of an n-link revolute manipulator with a prismatic end-effector for landmark navigation. *PeerJ Computer Science*, 8:e885:1–27, 2022.
- [28] S. A. Kumar, J. Vanualailai, B. Sharma, and A. Prasad. Velocity controllers for a swarm of unmanned aerial vehicles. *Journal of Industrial Information Integration*, 22:100198, 2021.
- [29] S. A. Kumar and J. Vanualailai. A Lagrangian UAV swarm formation suitable for monitoring exclusive economic zone and for search and rescue. In *Proceedings of the 2017 IEEE Conference on Control Technology and Applications*, pages 1874–1879, Kohala Coast, Hawaii, USA, August 2017.
- [30] A. Prasad, B. Sharma, J. Vanualailai, and S. A. Kumar. A geometric approach to target convergence and obstacle avoidance of a nonstandard tractor-trailer robot. *International Journal of Robust and Nonlinear Control*, 30(13):4924–4943, 2020.
- [31] A. Prasad, B. Sharma, J. Vanualailai, and S. A. Kumar. Stabilizing controllers for landmark navigation of planar robots in an obstacle-ridden workspace. *Journal of Advanced Transportation*, 2020, 2020.
- [32] S. A. Kumar, J. Vanualailai, and A. Prasad. Distributed velocity controllers of the individuals of emerging swarm clusters. In *2020 IEEE Asia-Pacific Conference on Computer Science and Data Engineering (CSDE)*, pages 1–6, 2020.
- [33] A. Prasad, B. Sharma, and S. A. Kumar. Strategic creation and placement of landmarks for robot navigation in a partially-known environment. In *2020 IEEE Asia-Pacific Conference on Computer Science and Data Engineering (CSDE)*, pages 1–6, 2020.